

Relationship between Processing Method and Microstructural and Mechanical Properties of Poly(ethylene terephthalate)/Short Glass Fiber Composites

N. M. L. Mondadori,¹ R. C. R. Nunes,² A. J. Zattera,¹ R. V. B. Oliveira,³ L. B. Canto²

¹Chemistry Engineering Department, Caxias do Sul University (UCS), Caxias do Sul, RS, Brazil

²Federal University of Rio de Janeiro (UFRJ), Institute of Macromolecules (IMA), Zip Code: 21945-970, PO Box 68525, Rio de Janeiro, RJ, Brazil

³Chemistry Institute, Federal University of Rio Grande do Sul (UFRGS), Porto Alegre, RS, Brazil

Received 13 March 2008; accepted 30 March 2008

DOI 10.1002/app.28459

Published online 23 May 2008 in Wiley InterScience (www.interscience.wiley.com).

ABSTRACT: Composites of recycled poly(ethylene terephthalate) (PET) reinforced with short glass fiber (GF) (0, 20, 30, and 40 wt %) were compounded in a single-screw extruder (SSE) and in a intermeshing corotating twin-screw extruder (TSE). An SSE fitted with a barrier double-flight screw melting section in between two single-flight sections and a TSE with a typical screw configuration for this purpose were used. The composites were subsequently injection molded at two different mold temperatures (10 and 120°C), with all other operative molding parameters kept constant. The effects of processing conditions on composite microstructure, PET degree of crystallinity, and composite mechanical properties were evaluated. Appropriate dispersive and distributive mixing of the glass fiber throughout the PET

matrix as well as fine composite mechanical and thermal-mechanical properties were achieved regardless of whether the composites were prepared in the SSE or TSE. The performance of the SSE was attributed to the efficiency of the barrier screw melting section in composite mixing. The mold temperature influenced the mechanical properties of the composites, by controlling of the degree of crystallinity of the PET in the composites. For a good balance of mechanical and thermal-mechanical properties, high mold temperatures are desirable, typically, 120°C for a mold cooling time of 45 s. © 2008 Wiley Periodicals, Inc. *J Appl Polym Sci* 109: 3266–3274, 2008

Key words: recycled PET; composite; short glass fiber single-screw extruder; twin-screw extruder

INTRODUCTION

Short glass fiber-reinforced poly(ethylene terephthalate) composites (PET/GF) have been widely used to manufacture injection-molded articles for domestic, electrical, and automotive applications where engineering properties such as high stiffness, strength, toughness, and thermal resistance are required. An understanding of the relationships between material processing and morphology, and how they affect the mechanical properties, is essential for the development of these composites.^{1–3}

The final morphology of the molded parts of the PET/GF composites is governed by the physico-chemical characteristics of the glass fiber and the thermoplastic, as well their relationship with the processing conditions. The degree of reinforcement by glass fiber addition will depend on aspect ratio (fiber length/diameter) and volume fraction in the

composite, fiber orientation and distribution through the thermoplastic matrix of the molded parts, and the adhesion between the fiber and the polymeric matrix. This adhesion is dependent on the surface chemistry of the fiber and on the presence of functional groups in the polymer. Another important aspect governing the reinforcement of this kind of composite is the semicrystalline morphology of the thermoplastic matrix, i.e., the spherulitic morphology and the degree of crystallinity, the degree of orientation of amorphous phase, and the skin-core thickness of molded parts. These two kinds of morphologies, that is, polymer/fiber and the semicrystalline nature of polymeric matrix, are usually interdependent.^{1–3}

Attempts to correlate raw material properties and processing conditions to the PET/GF performance have been reported in some articles.^{4–12} Particular attention has been given to composites based on recycled PET, due to the economical and environmental advantages of this recycled polymer.¹³ Giraldi et al.^{4,5} have correlated the mechanical properties with compounding conditions—screw speed and screw torque—for twin-screw compounded recycled

Correspondence to: L. B. Canto (lbcanto@ima.ufrj.br).

PET/GF composites. These studies have showed that higher values of screw speed or screw torque produce small increases in the modulus, impact strength and melt flow index (MFI) due to a better GF dispersion and lower PET degradation. Arencon and Velasco⁶ have correlated the microstructure and the mechanical properties of short glass fiber-reinforced PET composites with the injection molding variables mold temperature and cooling time. The authors showed that these variables play a decisive role in controlling the development of the PET matrix crystallinity, which is directly correlated with the values of tensile strength, elongation at break, and Vicat softening temperature.

The aim of this study is compare the performance of two types of extruder (single-screw extruder fitted with a barrier screw versus intermeshing corotating twin-screw extruder) as well as the mold temperature of the injection-molding process on ultimate microstructure, degree of crystallinity and mechanical and thermal-mechanical properties of PET reinforced with short glass fiber.

EXPERIMENTAL

Raw materials

Waste bottle-grade PET, in flake form, with intrinsic viscosity of 0.70 dL g^{-1} (ASTM D 4603), was used. The short glass fiber, supplied by Vetrotex Saint-Gobain Company, Brazil, under code EC 983, was E-glass roving of 4.5-mm chopped filaments with fiber diameter of $10 \text{ }\mu\text{m}$ and with an aminosilane sizing.

Extruder compounding

PET/GF composites with different amounts of glass fiber (0, 20, 30, and 40 wt %) were processed individually in two different types of extruder: single-screw extruder and intermeshing corotating twin-screw extruder. Prior to the processing, the PET and GF were dried in an air-circulating oven at 65°C for 48 h.

The single-screw extruder (SSE) ($L/D = 32$ and $D = 35 \text{ mm}$) was designed to provide high intensity mixing. The screw geometry is comprised of a barrier flight screw melting zone, in between single flight screw feed and metering zones. It was operated with a barrel temperature profile of $250\text{--}260\text{--}270\text{--}275^\circ\text{C}$ (from hopper to die) and screw speed of 50 rpm. The materials were formulated by introducing all the components simultaneously into the extruder hopper during a single processing step. The throughput was 8 kg h^{-1} at this condition.

The twin-screw extruder (TSE), a Werner and Pfleiderer modular intermeshing corotating model, with $L/D = 36$ and $D = 30 \text{ mm}$, was set with a

screw configuration comprising two kneading blocks (stagger angles of 45°) separated by a conventional conveying section. The set upstream contains fifteen right-hand kneading discs followed by a set of five left-hand kneading discs, whereas the set downstream is composed of ten right-hand kneading discs followed by a left-hand conveying element. The barrel temperature profile was set to be constant at 275°C and the screw speed at 200 rpm. The PET was fed into the hopper by a gravimetric feeder. Glass fiber was introduced into the molten PET by a side feeder at a location just before the second set of kneading blocks. The feed rate (PET + GF) was set from 10 to 15 kg h^{-1} to maintain the extruder torque level constant at 85%.

The extruded strands were quenched in a water bath, pelletized, and dried in air-circulating oven at 65°C for 48 h.

Injection molding

Specimens for mechanical tests (ASTM standard bars) were injection-molded from the extruded pellets using a HIMACO LH 150-80 at a barrel temperature of 280°C , holding pressure of 650 bar for 4 s, mold cooling time of 45 s and mold temperature of $(120 \pm 2)^\circ\text{C}$ (or $10 \pm 2)^\circ\text{C}$.

Scanning electron microscopy investigations

The microstructures of the PET/GF composites were investigated using a Jeol JSM 6060 scanning electron microscope (SEM) in the top of cryo-fractured injection-molded impact bars. The fractured surfaces were coated with gold using a diode sputtering coater before SEM observation.

Optical microscopy investigations

The average lengths (L_n) of the fibers in the composites were determined using a Nikon Epihot 200 optical microscope coupled with a DMX 1200F digital camera, and an Image Pro-Plus image analyzer, on about 400 fibers. The fibers were recovered from the injection-molded impact bars by burning off the PET at 600°C for 3 h.

Differential scanning calorimetry analysis

Differential scanning calorimetry (DSC) analysis was performed to determine the degree of crystallinity of the PET in the injection-molded bars. Scans from 20 to 300°C , with a heating rate of $10^\circ\text{C min}^{-1}$ and under N_2 atmosphere (50 mL min^{-1}), were carried out in a Shimadzu DSC-50 calorimeter. Samples ($\sim 10 \text{ mg}$) were taken from the inner part of the

injection-molded Izod bars. The degree of crystallinity of the PET (X_c) was calculated using eq. (1):

$$X_c = \frac{\Delta H_m - \Delta H_c}{\Delta H_f} \times 100\% \quad (1)$$

In eq. (1), ΔH_c is the cold crystallization enthalpy and ΔH_m is the melting enthalpy, which were calculated from the DSC thermograms, and ΔH_f is the heat of fusion of 100% crystalline PET (120 J g^{-1}).¹⁴

Mechanical tests

Tensile tests were performed on type I bars using an EMIC DL 2000 universal testing machine at a crosshead speed of 50 mm min^{-1} , according to ASTM D 638.

Flexural tests (three point bending) were carried out according to ASTM D 790, with a EMIC DL 2000 machine, at a crosshead speed of 2 mm min^{-1} .

Izod impact strength was measured with a Ceast Resil 25 pendulum using notched specimens, according to ASTM D 256.

Heat distortion temperature (HDT) tests were performed on a CEAST instrument under a load of 1.8 MPa and with a heating rate of 2°C min^{-1} , according to ASTM D 648.

The bars were conditioned at 23°C and 50% relative humidity for 48 h prior to the tests, which were all conducted under the same climatic conditions. Each mechanical test value was calculated as the average of at least five independent measurements. The standard deviations of each value were calculated and are shown as error bars in the plots.

RESULTS AND DISCUSSION

The scanning electron micrographs of cryo-fractured surfaces of PET/GF composites compounded in the two types of extruder (SSE and TSE) followed by injection molding are presented in Figure 1. For all the composites, good fiber wetting and an absence of fiber bundles were observed, which reveals appropriate dispersive and distributive mixing of the glass fiber throughout the PET matrix, as required to impart good mechanical properties. There was no apparent difference between the two extrusion processes or in the amount of fiber used.

The glass fiber length distributions in the PET/GF composites are shown in Figure 2. The average lengths (L_n) of the glass fibers obtained from the statistical data are shown in the Figure 2(a–f). For each PET/GF composite (a,b, c,d, e,f), similar fiber length distribution patterns were observed, irrespective of the manner in which the composites were processed (single- or twin-screw extruder). For all the composites, the fiber length reduction is more severe as

the fiber content increases in the composites, due to the increased fiber–fiber interactions during processing.³

The critical fiber length for composite reinforcement, $(L/D)_c$, can be deduced using eq. (2),¹⁵ which expresses the balance of force between the tensile strength of the fiber (σ_f) and the fiber-matrix interfacial shear strength (τ_{int}):

$$\left(\frac{L}{D}\right)_c = \frac{\sigma_f}{2\tau_{\text{int}}} \quad (2)$$

Assuming a perfect bonding between the fiber and the matrix, the interfacial shear strength becomes the shear strength of the polymer matrix, which is 45 MPa for PET.¹⁶ Taking a typical value for the fiber strength of 1500 MPa^2 , a critical fiber length of $167 \mu\text{m}$ is obtained for PET reinforcement.

Thus, for the composites under study the average fiber lengths (Fig. 2) are around 1.5–2.0 times the critical value for PET, which is essential for ensuring effective stress transfer from the PET matrix to the glass fibers as the composites are mechanically overloaded.

It is important to mention that although the microstructure of the PET/GF composites were evaluated from injection molded bars, it is reasonable to use the data to make a comparison between the performance of the two extruders that were used to compound the composites, since it is well-known that the extrusion is the step where the main fiber breakage takes place.³

The observations above show that the single-screw extrusion was able to generate a suitable level of mixing for preparation of PET/GF composites with an optimized microstructure, comparable with that of corotating twin-screw extruded samples.

The barrier screw melting section can be considered the key factor determining the performance of the SSE, since it is well-known that mixing in single-flight screws is poor.¹⁷ The barrier flight divides the main screw channel so that the melt pool is continuously separated from the solid bed along the screw section length. This melt separation enlarges the area of heat conduction between the solid bed and the screw barrel wall that increases the overall melting capacity¹⁷ and melt temperature homogeneity.¹⁸ In addition, as the melt pool is forced over the barrier it undergoes dispersive mixing.¹⁹

Therefore, for the PET/GF composites under study, the barrier melting section of the SSE is believed to increase the residence time in which glass fibers remain in contact with melted PET chains, thus maximizing the glass fiber dispersion and distribution throughout the PET. Moreover, although not measured here, some studies have shown that barrier screws are suitable for oxygen reduction in the molten polymer²⁰ and this could help to minimize

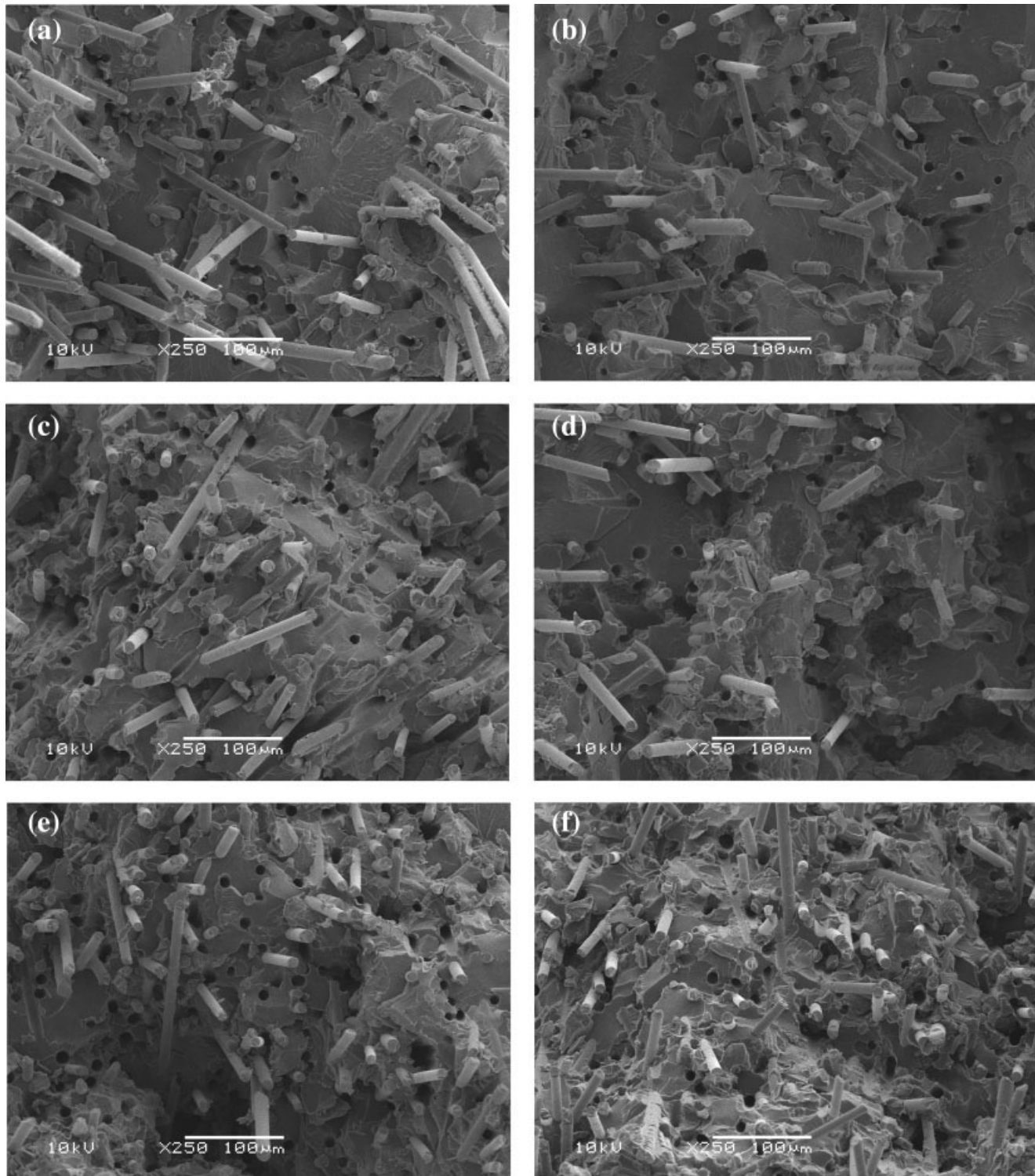


Figure 1 Scanning electron micrographs of cryo-fractured surfaces of injection molded PET/GF composites. Samples with varying compositions (20–40 wt % of GF, a–f) prepared using two types of extruder (SSE (a, c, e) and TSE (b, d, f)) and injection molded at mold temperature of 120°C.

the PET degradation during extrusion, which is an additional benefit.

Corotating twin-screw extruders are frequently preferred for compounding polymer composites

because they can generally provide more effective mixing than single screw extruders. However, the latter are generally less expensive and more readily available for commercial purposes. Thus, the per-

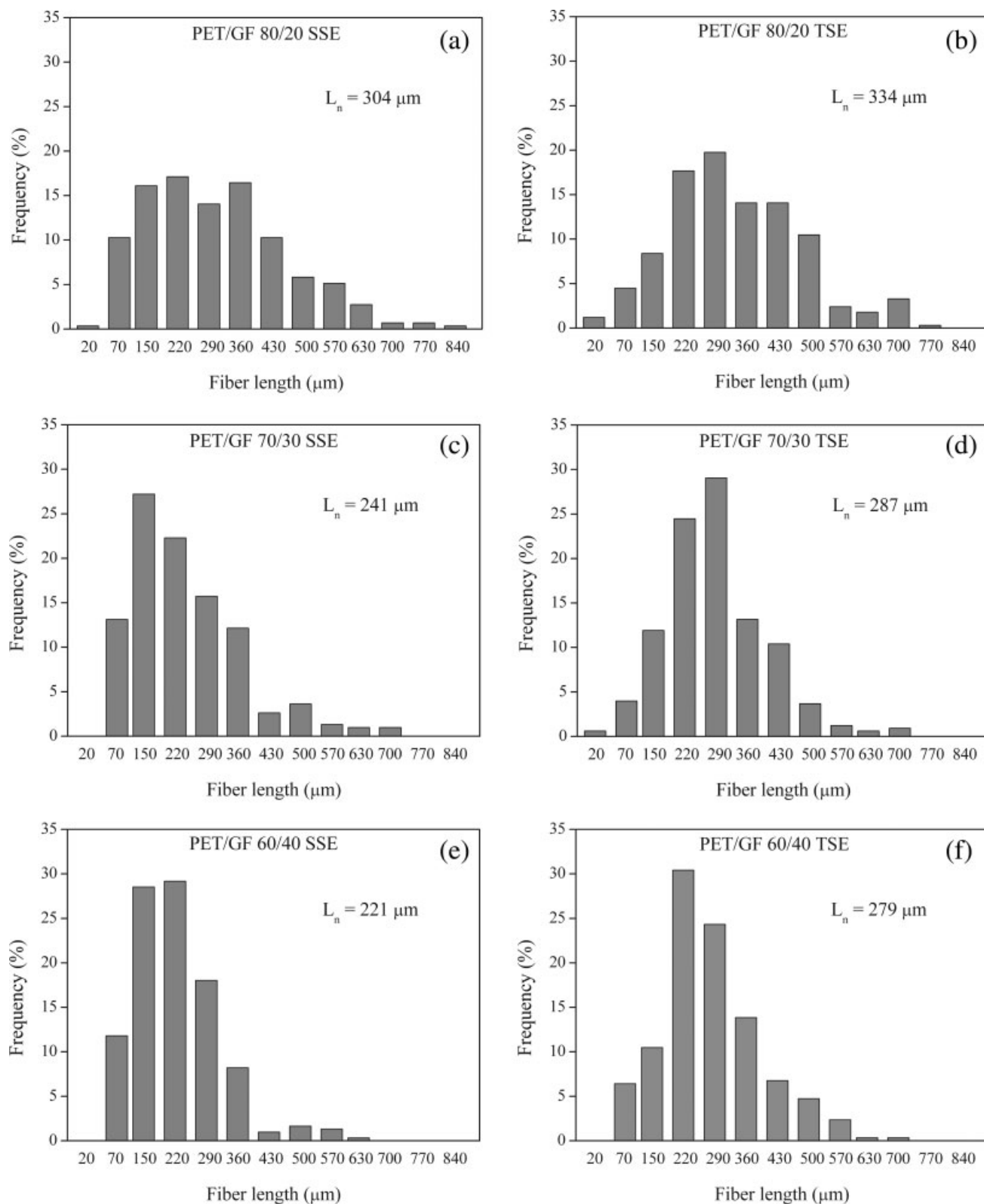


Figure 2 Glass fiber length distributions of injection molded PET/GF composites. Samples with varying compositions (20–40 wt % of GF, a–f) prepared using two types of extruder (SSE (a, c, e) and TSE (b, d, f)) and injection molded at mold temperature of 120°C.

formance of SSE in the PET/GF composites processing is in addition an interesting feature from a technological point of view.

Figure 3 shows the tensile modulus as a function of glass-fiber content for the composites processed in the SSE and in the TSE and injection molded at

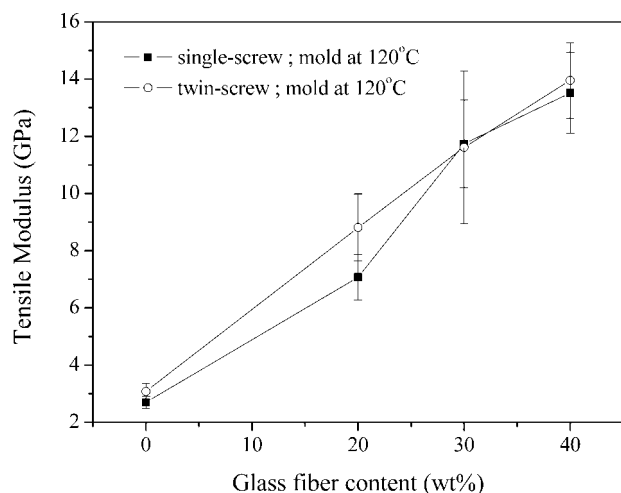


Figure 3 Tensile modulus of PET/GF composites. Samples with varying compositions (20–40 wt % of GF) prepared using two types of extruder (SSE and TSE) and injection molded at mold temperature of 120°C.

mold temperature of 120°C. The modulus values were found to increase almost monotonically with addition of GF. In addition, for each composition, practically no differences in the modulus were observed regardless of whether the composites were processed in the twin- or single-screw extruder.

According to the Halpin-Tsai model,²¹ the tensile modulus of a fiber-reinforced composite can be expressed in terms of the corresponding property of the matrix and the fiber phase together with their proportions and the fiber geometry, using eq. (3):

$$E_r = \frac{E_c}{E_m} = \frac{1 + \xi \cdot \eta \cdot \phi}{1 - \eta \cdot \phi} \quad \text{and} \quad \eta = \frac{(E_f/E_m - 1)}{(E_f/E_m + \xi)} \quad (3)$$

In eq. (3), E_r is the relative modulus and E_c , E_m , and E_f are, respectively, the moduli of the composite, matrix and fiber; ϕ is the fiber volume fraction.

The factor ξ of eq. (3) describes the influence of the geometry of the reinforcing phase. For oriented short fibers with aspect ratios higher than the critical value, the factor ξ assumes the form $\xi = 2 \cdot (L/D)_c$ for fibers oriented parallel to the stress/strain; and $\xi = 2$ for fibers oriented perpendicular to stress/strain.

The relative tensile modulus values for the composites processed in SSE and TSE and injection molded at mold temperature of 120°C are shown in Figure 4(a,b), along with the predictive values obtained according to the Halpin-Tsai model. In this analysis, the tensile module of the glass fiber was taken as 70 GPa.² As can be seen in Figure 4, the experimental tensile modulus values of the composites processed either in the SSE [Fig. 4(a)] or in the TSE [Fig. 4(b)] are very close to the maximum value, in which the

fibers are considered to be longitudinally oriented in relation to the applied strain. Such a behavior suggests a high level of fiber orientation in the injection-molded tensile bars.

Flexural modulus, flexural strength and impact strength values for the composites processed in SSE and TSE and injection molded at mold temperature of 120°C are shown in Figure 5(a–c).

The flexural modulus [Fig. 5(a)] and the flexural strength values [Fig. 5(b)] had similar behavior as the respective tensile modulus and strength values, that is, a linear increase with glass fiber content. Similar values were observed irrespective of the manner in which the composites were extruded, using SSE or TSE. The mechanical behavior under tensile and flexure modes attests to the effective PET reinforcement by the glass fiber provided by both extruder types. Such a mechanical performance is in

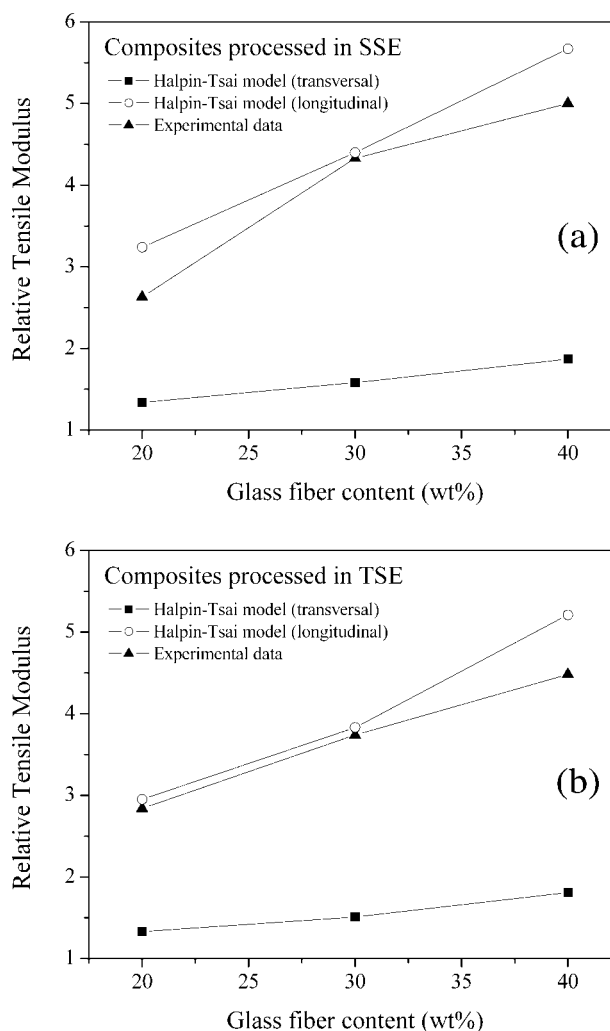


Figure 4 Relative tensile modulus of PET/GF composites processed in SSE (a) and TSE (b) and injection molded at mold temperature of 120°C along with the predicted values obtained according to the Halpin-Tsai model.

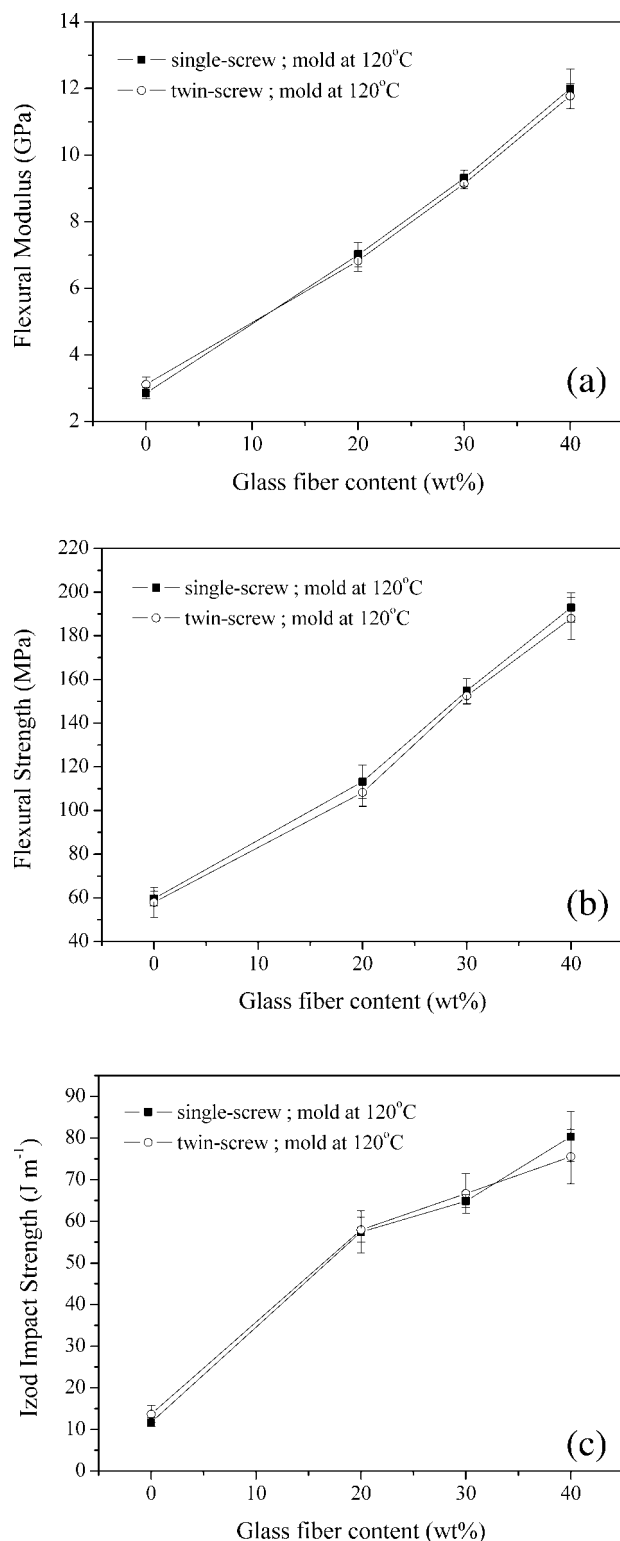


Figure 5 Flexural modulus (a), flexural strength (b) and notched Izod impact strength (c) of PET/GF composites processed in SSE and TSE and injection molded at mold temperature of 120°C.

agreement with the composite microstructures (Fig. 1) and the optimized glass fiber size distributions (Fig. 2) in the composites, and with the longitudinal

fiber orientation in the composite molded parts, as suggested by data from Figure 4.

The Izod impact strengths [Fig. 5(c)] were found to increase with fiber content. However, the improvement in impact strength was not linearly dependent on the amount of fiber, tending to level off for composites with more than 30 wt % glass fiber. This is to a certain extent predictable due to the constraining effect of neighboring fibers as the fiber volume is increased significantly. In fact, the mechanism of polymer matrix toughening using short glass fibers is distinct as compared to that of fiber reinforcement. For effective toughening fiber lengths shorter than the critical values are desired, since fibers are likely to debond from the matrix, and then to pull completely out of the matrix, allowing plastic deformation before failure. Of course, since there is a fiber length distribution in the molded composites, the presence of a proportion of short fibers is probably responsible for the observed toughness enhancement.³

Figure 6 shows the PET degree of crystallinity, as measured by DSC, in the PET/GF composites processed in SSE and TSE and injection molded at two different mold temperatures: 10 and 120°C. As expected, the mold temperature significantly influenced the degree of crystallinity of the PET in the injection-molded PET/GF composites. The higher mold temperature (120°C) led to a greater PET degree of crystallinity in the composites, regardless the extrusion method. Higher mold temperatures reduce the cooling rate during mold filling, hence allowing the PET chains to stay longer at around 165–175°C (temperature range where the rate of PET crystallization is at a maximum), facilitating the

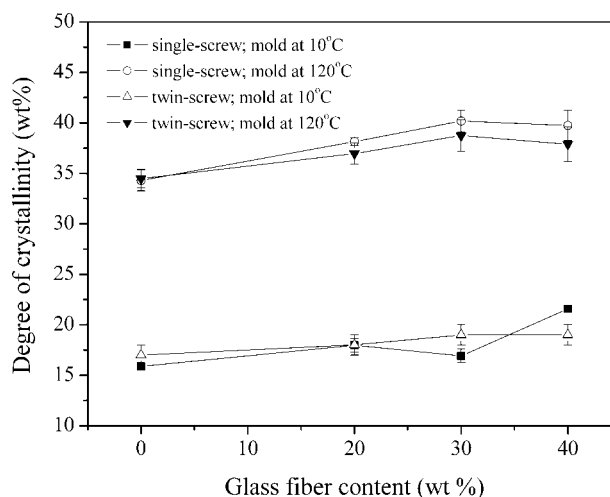


Figure 6 Degree of crystallinity of PET in the PET/GF composites processed in SSE and TSE and injection molded at two different mold temperatures (10 and 120°C).

spherulitic crystallization of PET and increasing the PET degree of crystallinity.²² In addition, small increases in the degree of crystallinity of PET were observed for composites with increasing amounts of GF up to 30 wt %, which suggests that GF acts as a nucleating agent for PET, in addition to its role as in reinforcement.

The PET degrees of crystallinity influenced the mechanical and thermal-mechanical performance of the composites. As the composites are injection-molded at low mold temperature (10°C) the impact strength is increased to some extent (Fig. 7). However, slightly lower modulus values are observed (Fig. 7) in addition to a dramatic decrease in the HDT (Fig. 8).

The observations relating to the mechanical properties as a function of PET crystallinity degree can be explained based on the individual behavior of the amorphous and the crystalline phases of semicrystalline PET. Higher crystallinity degrees result in a higher amount of densely packed chains, thus constraining the molecular motion and restricting plastic deformation. Hence, an increase in stiffness but a decrease in toughness is expected as the mold temperature is increased. With regard to the softening temperature, the amorphous phase of PET softens at temperatures close to T_g (70°C), whereas the crystalline phase softens at temperatures close to the melting temperature (255°C). Thus, depending on the relative fraction of amorphous and crystalline phases, the behavior of the HDT will be determined by one of these microstructures. Arencon and Velasco⁶ have previously shown a similar effect of the degree of crystallinity on the modulus and Vicat softening of glass fiber-reinforced PET composites. On the other hand, relationships between impact strength and

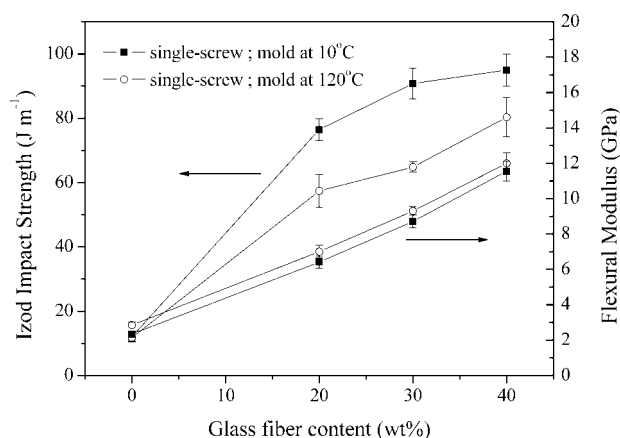


Figure 7 Notched Izod impact strength and flexural modulus of PET/GF composites. Samples with varying compositions (20–40 wt % of GF) prepared using SSE and injection molded at two different mold temperatures (10 and 120°C). Some graphical data of Figure 5(a,c) were enclosed for comparison.

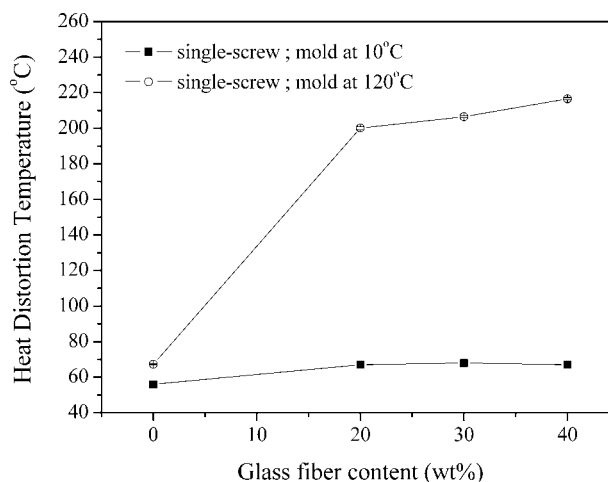


Figure 8 Heat distortion temperature (HDT) of PET/GF composites. Samples with varying compositions (20–40 wt % of GF) prepared using SSE and injection molded at two different mold temperatures (10 and 120°C).

degree of crystallinity have been explored using neat PET,²³ but an extension of these studies to PET composites containing glass-fiber has not been reported to date.

CONCLUSIONS

The studies here reported on short glass fiber-reinforced PET composites showed that a single-screw extruder with screw geometry containing a barrier double-flight screw melting section can replace successfully a corotating twin-screw extruder with a typical configuration for this purpose. Appropriate composite microstructure as well as fine mechanical and thermal-mechanical properties were achieved regardless of whether the composites were processed using the single-screw or twin-screw extruder. In injection molding, the mold temperature was observed to be an important parameter influencing the mechanical properties of PET/GF composites, by controlling of the degree of crystallinity of the PET in the PET/GF composites. For a good balance of mechanical properties, high mold temperature is desirable, typically 120°C for a mold cooling time of 45 s.

The authors thank FAPERGS-Brazil for the grant awarded to N. M. L. Mondadori and to Professor Elias Hage (UFSCar/Brazil) who kindly loaned the twin-screw extruder.

References

- Rosato, D. V.; Rosato, D. V. *Reinforced Plastics Handbook*, 3rd ed.; Elsevier Advanced Technology: Oxford, 2004.
- Chawla, K. K. *Composite Material Science and Engineering*, 2nd ed.; Springer-Verlag: New York, 1998.

3. Folkes, M. J. *Short Fibre Reinforced Thermoplastics*; Research Studies Press: New York, 1985.
4. Giraldi, A. L. F.; de M.; Bartoli, J. R.; Velasco, J. I.; Mei, L. H. I. *Polym Test* 2005, 24, 507.
5. Giraldi, A. L. F.; de M.; Jesus, R. C. de; Mei, L. H. I. *J Mater Process Tech* 2005, 162/163, 90.
6. Arencon, D.; Velasco, J. I. *J Thermoplast Compos Mater* 2002, 15, 317.
7. Cantwell, W. J. *J Reinforced Plast Compos* 1999, 18, 373.
8. Ronkay, F.; Czigany, T. *Polym Advan Technol* 2006, 17, 830.
9. Fung, K. L.; Li, R. K. Y. *Polym Test* 2006, 25, 923.
10. Pegoretti, A.; Penati, A. *Polymer* 2004, 45, 7995.
11. Takahashi, K.; Choi, N. S. *J Mater Sci* 1991, 26, 4648.
12. Kwok, K. W.; Choy, C. L.; Lau, F. P. *J Reinforced Plast Compos* 1997, 16, 290.
13. Awaja, F.; Pavel, D. *Eur Polym J* 2005, 41, 1453.
14. Metha, A.; Wunderlich, B. *J Polym Sci Polym Phys* 1978, 16, 289.
15. Kelly, A.; Tyson, W. R. *J Mech Phys Solids* 1965, 13, 329.
16. Luethia, B.; Rebera, R.; Mayera, J.; Wintermantela, E.; Janczak-Ruschb, J.; Rohrb, L. *Compos A* 1988, 29, 1553.
17. MacGregor, A.; Vlachopoulos, J.; Vlcek, J. *J Reinforced Plast Compos* 1997, 16, 1270.
18. Kelly, A. L.; Brow, E. C.; Coates, P. D. *Polym Eng Sci* 2006, 46, 1706.
19. Rauwendaal, C. *Polymer Extrusion*, 4th ed.; Hanser Gardner Publications: Ohio, 2001.
20. Kometani, H.; Matsumura, T.; Suga, T.; Kanai, T. *Int Polym Proc* 2006, 21, 24.
21. Halpin, J. C.; Kardos, J. L. *Polym Eng Sci* 1976, 16, 344.
22. Viana, J. C.; Alves, N. M.; Mano, J. F. *Polym Eng Sci* 2004, 44, 2174.
23. Torres, N.; Robin, J. J.; Boutevin, B. *Eur Polym J* 2000, 36, 2075.